

# Effect of Mixing of Metal Cations on the Topology of Metal Oxide Networks\*\*

Carine Livage,\* Paul M. Forster, Nathalie Guillou, Maya M. Tafoya, Anthony K. Cheetham, and Gérard Férey

Most of the porous hybrid metal–organic frameworks (MOFs) discovered up to now are coordination polymers in which metal atoms or inorganic clusters are bridged by polyfunctional organic molecules.<sup>[1–7]</sup> However, some hybrids have inorganic subnetworks in which metal–oxygen–metal bonds extend in one, two, or even three dimensions. The closer resemblance of such extended inorganic hybrids<sup>[8]</sup> to metal oxides implies that, compared to coordination polymers, they may be more likely to show analogous properties such as long-range magnetic ordering<sup>[9–11]</sup>. However, examples of three dimensional (3D) metal–oxygen–metal arrays are scarce and, to our knowledge, only two architectures have been described with dicarboxylates (nickel succinate and nickel glutarate),<sup>[10,12]</sup> two with monocarboxylates (formate, acetate),<sup>[13–15]</sup> and one with an amino acid (aspartate).<sup>[16]</sup> These examples show that 3D inorganic MOFs are more specific to small, flexible carboxylates.<sup>[17]</sup>

Previously, we studied relations between synthetic parameters (metal/succinate ratio, pH, concentration) and observed architectures for cobalt and nickel succinates.<sup>[17,18]</sup> In the case of cobalt, we demonstrated that condensation of the inorganic species increased with increasing temperature and pH, and this led to seven cobalt succinate topologies.<sup>[18]</sup> Comparison of these compounds to known nickel succinates indicates that the phases that occur at lower temperatures tend to be isostructural (consistent with other Co<sup>II</sup> and Ni<sup>II</sup> coordination polymers)<sup>[19,20]</sup> while the hydrothermal phases differ significantly. In particular conditions used for synthesizing the cobalt structure MIL-9,<sup>[21–23]</sup> which exhibits a 2D array of metal octahedra, gave a remarkable 3D

inorganic framework when applied to nickel.<sup>[12]</sup> These observations suggest that a hydrothermal study of the Co/Ni ratio as sole reaction variable may improve our understanding of the relationship between these two systems.

In MIL-9, Co<sub>5</sub>(OH)<sub>2</sub>(C<sub>4</sub>H<sub>4</sub>O<sub>4</sub>)<sub>4</sub>, Co<sup>II</sup> occupies five crystallographic sites with the same multiplicity. Consequently, we increased the ratio of Ni<sup>II</sup> in increments of 20 %, corresponding to substitution at each potential site. The starting mixture with a molar ratio of (M, M')Cl<sub>2</sub>:1.5succinic acid:3 KOH:120H<sub>2</sub>O was heated to 180 °C. The resulting series contained four crystalline phases. As illustrated in Figure 1, at 20 % Ni substitution in **1**, the major phase becomes M<sub>4</sub>(OH)<sub>2</sub>-

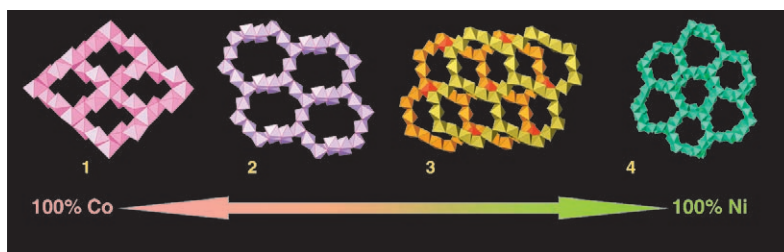


**Figure 1.** Progressive formation of the four phases starting from Co succinate Co<sub>5</sub>(OH)<sub>2</sub>(C<sub>4</sub>H<sub>4</sub>O<sub>4</sub>)<sub>4</sub> (**1**) with increasing substitution by Ni: M<sub>4</sub>(OH)<sub>2</sub>(H<sub>2</sub>O)<sub>2</sub>-(C<sub>4</sub>H<sub>4</sub>O<sub>4</sub>)<sub>3</sub>·2H<sub>2</sub>O (**2**), M<sub>7</sub>(OH)<sub>2</sub>(H<sub>2</sub>O)<sub>2</sub>(C<sub>4</sub>H<sub>4</sub>O<sub>4</sub>)<sub>6</sub>·3.5H<sub>2</sub>O (**3**), and Ni<sub>7</sub>(OH)<sub>2</sub>(H<sub>2</sub>O)<sub>2</sub>-(C<sub>4</sub>H<sub>4</sub>O<sub>4</sub>)<sub>6</sub>·2H<sub>2</sub>O (**4**).

(H<sub>2</sub>O)<sub>2</sub>(C<sub>4</sub>H<sub>4</sub>O<sub>4</sub>)<sub>3</sub>·2H<sub>2</sub>O (**2**). This compound, already reported in its pure cobalt form,<sup>[24]</sup> is constructed by stacking of perforated metal oxide layers with hydrated 14-membered ring channels. When nickel becomes predominant, **2** is replaced by M<sub>7</sub>(OH)<sub>2</sub>(H<sub>2</sub>O)<sub>2</sub>(C<sub>4</sub>H<sub>4</sub>O<sub>4</sub>)<sub>6</sub>·3.5H<sub>2</sub>O (**3**), a previously unknown structure with an unprecedented 3D M–O–M topology (see below). With increasing nickel content up to 80 %, M<sub>7</sub>(OH)<sub>2</sub>(H<sub>2</sub>O)<sub>2</sub>(C<sub>4</sub>H<sub>4</sub>O<sub>4</sub>)<sub>6</sub>·2H<sub>2</sub>O (**4**) becomes the major phase. This topology, which was the first metal dicarboxylate with a 3D nickel oxide network, has layers in which 12- and 15-membered rings are connected through isolated octahedra.<sup>[12]</sup> When looking at the reduced chemical formula of **1–4**, some trends specific to the introduction of Ni appear. The number of succinate ligands L per metal center increases slightly for the nickel-rich compounds with a concomitant decrease in the degree of “hydrolysis” (μ-OH). Moreover, introduction of Ni increases the dimensionality of the inorganic network and decreases the density (Table 1).

While it is intuitive that hydrolysis-favoring synthesis conditions, such as an increase of pH or temperature, lead to increased inorganic condensation, it is more difficult to

[\*] Dr. C. Livage, Dr. N. Guillou, Prof. G. Férey  
Institut Lavoisier, UMR-CNRS 8180  
Université de Versailles Saint-Quentin-en-Yvelines  
45 avenue des Etats-Unis, 78035 Versailles Cedex (France)  
Fax: (+33) 1-3925-4358  
E-mail: livage@chimie.uvsq.fr

Dr. P. M. Forster  
Mineral Physics Institute, 255 Earth and Space Sciences  
Stony Brook University, Stony Brook, NY 11794-2100 (USA)  
M. M. Tafoya, Prof. A. K. Cheetham  
Materials Research Laboratory, University of California  
Santa Barbara, CA 93106 (USA)

[\*\*] This work was partially supported by the MRL program of the National Science Foundation under Award No. DMR00-80034.

Supporting information for this article is available on the WWW under <http://www.angewandte.org> or from the author.

**Table 1:** Reduced formulas (i.e., one metal atom per formula unit), calculated density, and calculated solvent-accessible voids for as-synthesized and dehydrated solids **1–4**.

	Reduced formula	Dimens. <sup>[a]</sup>	Density [g cm <sup>-3</sup> ] <sup>[b]</sup>	Calculated accessible voids [%] <sup>[c]</sup>
<b>1</b>	[M(OH) <sub>0.4</sub> L <sub>0.8</sub> ] <sup>[21]</sup>	2	2.337(5)	< 1
<b>2</b>	[M(OH) <sub>0.5</sub> (H <sub>2</sub> O) <sub>0.5</sub> L <sub>0.75</sub> ](H <sub>2</sub> O) <sub>0.5</sub> <sup>[24]</sup>	2	2.085(3)	2.3–13.8
<b>3</b>	[M(OH) <sub>0.28</sub> (H <sub>2</sub> O) <sub>0.28</sub> L <sub>0.86</sub> ](H <sub>2</sub> O) <sub>0.5</sub>	3	2.090(8)	7.0–11.2
<b>4</b>	[M(OH) <sub>0.28</sub> (H <sub>2</sub> O) <sub>0.28</sub> L <sub>0.86</sub> ](H <sub>2</sub> O) <sub>0.28</sub> <sup>[12]</sup>	3	1.995(8)	7.8–18.1

[a] Dimensionality of the inorganic subnetwork. [b] Deviation corresponds to the difference of 0.6% in atomic weight between Co and Ni. [c] PLATON geometric analysis and plotting program.<sup>[26]</sup>

explain the remarkable structural variations induced here by Co/Ni substitution as sole reaction variable. Surprisingly, in the pure cobalt system, when temperature is the only synthetic variable, the initial topology **1** crystallizes at 250 °C, whereas **2** only needs 150 °C.<sup>[25]</sup> Addition of nickel therefore has the same apparent effect as a lower temperature. However, the role of temperature was tested for **3**, and heating did not influence the nature of the final product (180–240 °C).

Following its isolation, synthesis conditions for **3** were optimized in order to obtain a pure phase with high crystallinity. Chemical analyses on several samples support a statistical distribution of Co and Ni within the structure and a Co/Ni ratio that varies from 1/1 to 1/2 independently of the initial composition. Figure 2c shows the 3D extended array of metal polyhedra, generated by eight independent metal sites, two of which are located on an inversion center. All metal atoms are octahedrally coordinated by oxygen atoms with bond lengths between 2.03 and 2.19 Å. As illustrated in Figure 2b, honeycomb sheets of edge-sharing octahedra are

connected by single corner-sharing octahedra. The metal network adopts a “distorted” diamond-like topology (Figure 2d).<sup>[5]</sup> Such layers were already observed for cobalt succinate and manganese glutarate.<sup>[17,27]</sup> Most of the structural characteristics of **3** correspond to features from either the more Co-rich **2**, in which the sheets are identical, and Ni-rich **4**, in which single octahedra connect sheets in the same way. The six crystallographically independent succinate anions act as scaffolds for the stability of the network. Free water molecules are located in pores formed by 14-octahedra rings and lined by the alkyl chains of dicarboxylates (Figure 2a).

Thermogravimetric studies showed a weight loss at 50 °C corresponding to the departure of the free water molecules, followed by the loss of coordinated water molecules at 220 °C. The second weight loss is associated with a change of color from light violet to green. Decomposition occurs around 300 °C under flowing oxygen and 380 °C under pure nitrogen.<sup>[28]</sup> Thermogravimetry performed under air showed three successive crystallographic changes at 50, 220, and 270 °C. Whereas this compound exhibits a reversible dehydration/rehydration process, crystallographic modifications observed with the departure of occluded water molecules certainly induce structural changes associated with loss of porosity. Indeed, for samples activated at 50, 100, or 180 °C under vacuum, no measurable surface area was obtained.

In spite of the extended M–O–M connectivity, magnetic susceptibility measurements revealed paramagnetic behavior down to 5 K. The best linear fit yielded  $C = 19.0 \text{ emu K mol}^{-1}$  and  $\theta = -50 \text{ K}$ . This gives a magnetic moment of  $4.66 \mu_B$  per metal atom, which is intermediate between the observed values for octahedral cobalt ( $5.2\text{--}5.5 \mu_B$ ) and nickel succinates ( $2.8\text{--}3.3 \mu_B$ ). The negative sign of  $\theta$  and a small decrease of  $\chi_{mT}$  versus  $T$  from room temperature to 50 K suggests antiferromagnetic interactions between metal centers. Below 50 K, an increase in susceptibility can be accounted for by assuming heterometallic occupation of the metal sites, which avoids compensation of magnetic moments.

In conclusion, this study has shown that a set of appropriate mixtures of metal ions allows synthesis of different solids with new unforeseen architectures. These results underline once more the difficulty of predicting or controlling inorganic condensation in the field of MOFs.<sup>[29]</sup> Acidobasic characteristics of cobalt and nickel are usually considered to be slightly different, but under hydrothermal conditions this difference seems to be enhanced and leads to different structural types. However, structural characteristics from previously characterized cobalt and nickel succinates dominate the new topology. Indeed, **3** is built up from the honeycomb layers of MIL-16, connected by isolated vertex-sharing octahedra typical of the 3D nickel succinate compound.

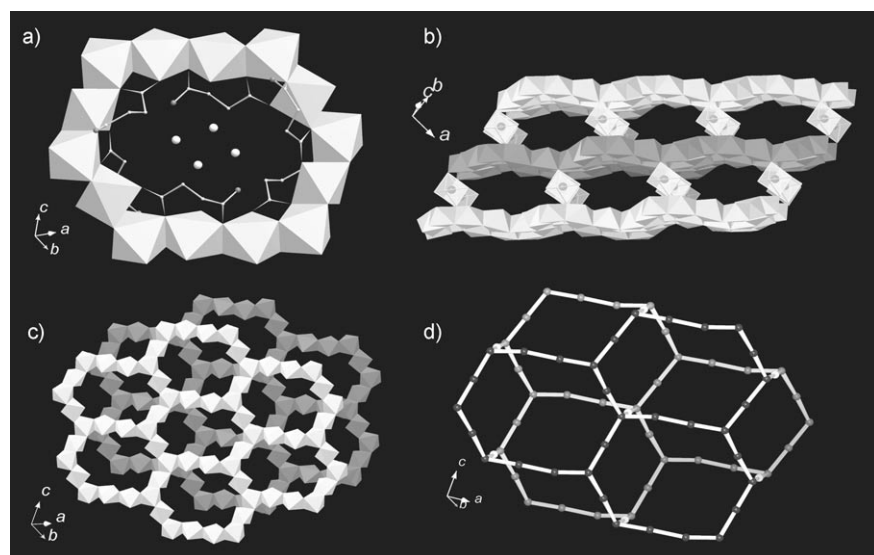


**Figure 2.** a) Polyhedral view of the 14-membered ring lined with succinate ions. b) Connection of the honeycomb layers by vertex-sharing metal octahedra. c) View perpendicular to the honeycomb sheets. d) Schematic representation of the metal network highlighting the distorted diamond-like topology (only metal atoms are shown).

## Experimental Section

Preparation of **3** was optimized, and it can be obtained as a pure phase with high crystallinity. A mixture containing  $\text{CoCl}_2 \cdot 6\text{H}_2\text{O}$  ( $2.3 \times 10^{-3}$  mol),  $\text{NiCl}_2 \cdot 6\text{H}_2\text{O}$  ( $2.3 \times 10^{-3}$  mol),  $\text{HO}_2\text{C}(\text{C}_2\text{H}_4)\text{CO}_2\text{H}$  ( $6.9 \times 10^{-3}$  mol),  $\text{KOH}$  ( $10.4 \times 10^{-3}$  mol), and  $\text{H}_2\text{O}$  (5 mL) corresponding to a molar ratio of 0.5:0.5:1.5:2.25:60 was heated at  $180^\circ\text{C}$  for 2 d. In contrast to the preparation of microcrystalline powder and in spite of many trials, single crystals were obtained only once and as minor product. The identity of these two samples was evidenced by Rietveld refinement of X-ray powder diffraction data with the structural model obtained from single-crystal data. IR for **3** (KBr pellet):  $\tilde{\nu} = 3549$  (w), 3493 (s),  $3422\text{ cm}^{-1}$  (s) ( $\nu(\text{OH})$  of OH and  $\text{H}_2\text{O}$ ); 1624–1573 (s) and 1435–1399 (s) (symmetric and asymmetric stretching bands of carboxylate groups). Single-crystal diffraction data were collected on a Bruker SMART CCD system with  $\text{MoK}_\alpha$  radiation ( $\lambda = 0.71073\text{ \AA}$ ). Intensity data were collected in 1271 frames with  $\omega$  scans (width of  $0.30^\circ$  and exposure time of 30 s per frame). Data reduction was performed with the SAINT software and absorption corrections by using the SADABS program.<sup>[30]</sup>  $\mu(\text{MoK}_\alpha) = 2.985\text{ mm}^{-1}$ ,  $F(000) = 1244$ ,  $2\theta_{\text{max}} = 56.6^\circ$ ; 20 128 reflections collected, of which 9042 were unique ( $R_{\text{int}} = 0.0733$ ). Final  $R$  indices ( $I > 2\sigma I$ ):  $R_1 = 0.0420$ ,  $wR_2 = 0.1057$ . Lorentzian and polarization corrections were made, the structure was solved by using direct methods and difference Fourier calculations, and the data were refined against  $|F^2|$  by using the SHELXTL suite.<sup>[31]</sup> All non-hydrogen atoms were refined anisotropically except for those of the free water molecules. Hydrogen atoms of the organic molecules were placed in calculated positions. CCDC 620466 contains the supplementary crystallographic data for this paper. These data can be obtained free of charge from The Cambridge Crystallographic Data Centre via [www.ccdc.cam.ac.uk/data\\_request/cif](http://www.ccdc.cam.ac.uk/data_request/cif). Crystallographic data for **3**:  $\text{C}_{24}\text{H}_{37}\text{M}_7\text{O}_{31.5}$ , triclinic, space group  $P\bar{1}$ ,  $a = 10.215(5)$ ,  $b = 11.271(5)$ ,  $c = 17.523(8)\text{ \AA}$ ,  $\alpha = 91.123(8)^\circ$ ,  $\beta = 95.620(8)^\circ$ ,  $\gamma = 100.987(8)^\circ$ ,  $V = 1969(1)\text{ \AA}^3$ ,  $Z = 2$ ,  $\rho_{\text{calcd}} = 2.090\text{ g cm}^{-3}$ .

Received: January 18, 2007

Revised: May 29, 2007

Published online: July 3, 2007

**Keywords:** cobalt · hydrothermal synthesis · metal–organic frameworks · nickel · porous materials

- [1] S. R. Batten, R. Robson, *Angew. Chem.* **1998**, *110*, 1558–1595; *Angew. Chem. Int. Ed.* **1998**, *37*, 1460–1494.
- [2] M. J. Rosseinsky, *Microporous Mesoporous Mater.* **2004**, *73*, 15–30.
- [3] S. Kitagawa, R. Kitaura, S.-I. Noro, *Angew. Chem.* **2004**, *116*, 2388–2430; *Angew. Chem. Int. Ed.* **2004**, *43*, 2334–2375.
- [4] G. Férey, *Chem. Mater.* **2001**, *13*, 3084–3098.
- [5] N. W. Ockwig, O. Delgado-Friedrichs, M. O’Keeffe, O. M. Yaghi, *Acc. Chem. Res.* **2005**, *38*, 176–182.
- [6] O. M. Yaghi, M. O’Keeffe, N. W. Ockwig, H. K. Chae, M. Eddaoudi, J. Kim, *Nature* **2003**, *423*, 705–714.
- [7] C. N. R. Rao, S. Natarajan, R. Vaidhyanathan, *Angew. Chem.* **2004**, *116*, 1490–1521; *Angew. Chem. Int. Ed.* **2004**, *43*, 1466–1496.
- [8] A. K. Cheetham, C. N. R. Rao, R. K. Feller, *Chem. Commun.* **2006**, 4780–4795.
- [9] Y. Kim, Y. Park, D. Y. Jung, S. Oh, D. S. Kim, J. C. Sur, *Chem. Lett.* **2004**, *33*, 230–231.
- [10] N. Guillou, C. Livage, M. Drillon, G. Férey, *Angew. Chem.* **2003**, *115*, 4137–4141; *Angew. Chem. Int. Ed.* **2003**, *42*, 5314–5317.
- [11] K. Barthelet, J. Marrot, D. Riou, G. Férey, *Angew. Chem.* **2002**, *114*, 291–294; *Angew. Chem. Int. Ed.* **2002**, *41*, 281–284.
- [12] P. M. Forster, A. K. Cheetham, *Angew. Chem.* **2002**, *114*, 475–477; *Angew. Chem. Int. Ed.* **2002**, *41*, 457–459.
- [13] D. N. Dybtsev, H. Chun, S. H. Yoon, D. Kim, K. Kim, *J. Am. Chem. Soc.* **2004**, *126*, 32–33.
- [14] R. Kuhlman, G. L. Schimek, J. W. Kolis, *Inorg. Chem.* **1999**, *38*, 194–196.
- [15] M. Vortelhaus, P. Adler, R. Clérac, C. E. Anson, A. K. Powell, *Eur. J. Inorg. Chem.* **2005**, 692–703.
- [16] E. V. Anokhina, Y. B. Go, Y. Lee, T. Vogt, A. J. Jacobson, *J. Am. Chem. Soc.* **2006**, *128*, 9957–9962.
- [17] N. Guillou, C. Livage, G. Férey, *Eur. J. Inorg. Chem.* **2006**, 4963–4978.
- [18] P. M. Forster, N. Stock, A. K. Cheetham, *Angew. Chem.* **2005**, *117*, 7780–7784; *Angew. Chem. Int. Ed.* **2005**, *44*, 7608–7611.
- [19] A. Beghidja, P. Rabu, G. Rogez, R. Welter, *Chem. Eur. J.* **2006**, *12*, 7627–7638.
- [20] F.-T. Xie, L.-M. Duan, J.-Q. Xu, L. Ye, Y.-B. Liu, X.-X. Hu, J.-F. Song, *Eur. J. Inorg. Chem.* **2004**, 4375–4379.
- [21] C. Livage, C. Egger, M. Nogués, G. Férey, *J. Mater. Chem.* **1998**, *8*, 2743–2747.
- [22] Y. J. Kim, D.-Y. Jung, K.-P. Hong, G. Demazeau, *Solid State Sci.* **2001**, *3*, 837–846.
- [23] Y. Kim, E. Lee, D. Y. Jung, *Bull. Korean Chem. Soc.* **1999**, *20*, 827–829.
- [24] C. Livage, C. Egger, G. Férey, *Chem. Mater.* **1999**, *11*, 1546–1550.
- [25] P. M. Forster, A. R. Burbank, C. Livage, G. Férey, A. K. Cheetham, *Chem. Commun.* **2004**, 368–369.
- [26] A. L. Spek, *Acta Crystallogr. Sect. A* **1990**, *46*, C34.
- [27] Y. Kim, Y. Park, D.-Y. Jung, *Inorg. Chem. Commun.* **2004**, *7*, 347–349.
- [28] Thermogravimetric analysis of  $[\text{M}_7(\text{OH})_2(\text{H}_2\text{O})_2(\text{C}_4\text{H}_4\text{O}_4)_6] \cdot 3.5\text{H}_2\text{O}$  was performed under flowing nitrogen. A gradual weight loss before  $120^\circ\text{C}$  corresponds to the presence of occluded water molecules (found: 4.6 wt %, calcd: 5.1 wt %). Then the loss of coordinated water was observed between  $120$  and  $180^\circ\text{C}$  (found: 2.9 wt %, calcd: 2.9 wt %). Combustion of the organic moiety begun around  $300^\circ\text{C}$  (found: 47.4 wt %, calcd: 48.3 wt %).
- [29] M. Jansen, J. C. Schön, *Angew. Chem.* **2006**, *118*, 3484–3490; *Angew. Chem. Int. Ed.* **2006**, *45*, 3406–3412.
- [30] G. M. Sheldrick, SADABS, Version 2.06, Empirical absorption correction program, University of Göttingen, Göttingen, Germany, **2002**.
- [31] G. M. Sheldrick, SHELXS97 and SHELXL97, Software package for crystal structure determination, University of Göttingen, Germany, **1997**.